

Emergence of Large Scale Structure in Barotropic β -Plane Turbulence

Nikolaos A. Bakas* and Petros J. Ioannou†

Department of Physics, National and Kapodistrian University of Athens, Panepistimiopolis, Zografos, Athens 15784, Greece
(Received 28 November 2012; published 29 May 2013)

In this Letter, we use a nonequilibrium statistical theory, the stochastic structural stability theory (SSST), to show that an extended version of this theory can make predictions for the formation of nonzonal as well as zonal structures (lattice and stripe patterns) in forced homogeneous turbulence on a barotropic β plane. Comparison of the theory with nonlinear simulations demonstrates that SSST predicts the parameter values for the emergence of coherent structures and their characteristics (scale, amplitude, phase speed) as they emerge and at finite amplitude. It is shown that nonzonal structures (lattice states or zonons) emerge at lower energy input rates of the stirring compared to zonal flows (stripe states) and their emergence affects the dynamics of jet formation.

DOI: [10.1103/PhysRevLett.110.224501](https://doi.org/10.1103/PhysRevLett.110.224501)

PACS numbers: 47.27.eb, 47.20.Ky, 47.27.De, 52.35.Mw

Turbulence in planetary atmospheres and in plasma flows is observed to be organized into large scale zonal jets with long-lasting coherent eddies or vortices embedded in them [1–4]. The jets control the transports of heat and chemical species in planetary atmospheres and separate the high temperature plasma from the cold containment vessel wall in magnetic plasma confinement devices. It is therefore important to understand the mechanisms for the emergence, equilibration, and maintenance of these coherent structures and the simplest model for this purpose is barotropic dynamics on a β plane. In this Letter, we present a theory that predicts the formation and nonlinear equilibration of large scale coherent structures in barotropic β -plane turbulence and then test this theory against nonlinear simulations.

A large number of numerical simulations of this model have shown that robust, large scale zonal jets emerge in the flow and are sustained at finite amplitude [5–9]. In addition, large scale westward propagating coherent waves that were called satellite modes or zonons were found to coexist with the zonal jets [8,10,11]. The emergence of jets has been described in terms of an anisotropic inverse energy cascade [6,12,13], or in terms of inhomogeneous mixing of vorticity [14,15], or in terms of a direct transfer of energy from small scale waves into the zonal jets, either through nonlinear interactions between finite amplitude Rossby waves [16,17] or through shear straining of the small scale waves by the jet [18]. However, the mechanism for the emergence and maintenance of nonzonal structures remains elusive. Statistical equilibrium theory applied in the absence of forcing and dissipation has been able to predict both jets and coherent vortices as maximum entropy structures [19], and a recent study has shown correspondence of the theoretical results with nonlinear simulations in the limit of weak forcing and dissipation [20]. Nevertheless, the relevance of these results in planetary and plasma flows that are strongly forced and dissipated and are therefore out of equilibrium remains to be shown.

In this Letter, we present results based on an extension of a nonequilibrium statistical theory, the stochastic structural stability theory (SSST) [21–23] or equivalently the second order cumulant expansion theory (CE2) [24–26]. While recent studies have demonstrated that SSST can predict the structure of zonal flows in turbulent fluids [25,27,28], the results presented in this Letter demonstrate that the extended version of SSST can predict the emergence of both zonal and nonzonal coherent structures and can capture their finite amplitude manifestations. In addition, we show that the extended version of SSST can also capture the disruption of jet formation caused by the presence of nonzonal structures, which was recently hypothesized in studies comparing the predictions of SSST with nonlinear simulations [25,27,28]. The emergence of nonzonal and zonal structures described above is similar to formation of the lattice and stripe patterns in homogeneous thermal nonequilibrium systems [29]. The analogy between the formation of stripes and zonal jets has been recently emphasized using SSST dynamics [30]. In this Letter we formulate the dynamics that can produce lattice states in turbulent flows.

Consider the stochastically forced barotropic vorticity equation on a plane tangent to the surface of a planet:

$$\partial_t \zeta + \psi_x \zeta_y - \psi_y \zeta_x + \beta \psi_x = -r\zeta - \nu \Delta^2 \zeta + f. \quad (1)$$

The relative vorticity is $\zeta = \Delta \psi$, ψ is the stream function, $\Delta = \partial_{xx}^2 + \partial_{yy}^2$ is the Laplacian, x is in the zonal (east-west) direction, and y is in the meridional (north-south) direction, $\beta = 2\Omega \cos \phi_0 / R$ is the gradient of planetary vorticity at latitude ϕ_0 , Ω is the rotation rate, and R the radius of the planet. Equation (1) is a good approximation for the dynamics of nondivergent motions at the mid latitudes of the planet and is also the infinite effective Larmor radius limit of the Charney-Hasegawa-Mima equation that governs drift-wave turbulence in plasmas. The effects of baroclinicity and divergence have been neglected for simplicity, but can be easily incorporated as in previous

SSST studies for the emergence and equilibration of jets in the outer planets [31] and in drift-wave turbulence [32]. We are assuming linear damping with coefficient r representing the Ekman drag induced by the horizontal boundaries and hyperdiffusion with coefficient ν that dissipates the energy flowing into unresolved scales. The forcing term f is necessary to sustain turbulence, and may parametrize processes that have not been included in the dynamics, such as forcing from small scale convection. In many previous studies, this excitation was taken as a temporally delta correlated and spatially homogeneous and isotropic random stirring. We follow the same forcing protocol and consider an isotropic ring forcing, injecting energy at rate ε in a narrow ring of wave numbers of width ΔK_f around the total wave number K_f .

We solve (1) in the doubly periodic domain $2\pi \times 2\pi$. The calculations in this Letter are with $\beta = 10$, $r = 0.01$, $\nu = 2 \times 10^{-6}$, $K_f = 8$, and $\Delta K_f = 1$. To illustrate the characteristics of the turbulent flow and the emergence of coherent structures, we consider two indices. The first is the zonal mean flow (zmf) index [25] defined as the ratio of the energy of zonal jets over the total energy, $\text{zmf} = \sum_{l:|l| < K_f} \hat{E}(k=0, l) / \sum_{kl} \hat{E}(k, l)$, where \hat{E} is the time averaged energy power spectrum of the flow and k, l are the zonal and meridional wave numbers, respectively. The second is the nonzonal mean flow (nzmf) index defined as the ratio of the energy of the nonzonal modes with scales lower than the scale of the forcing over the total energy: $\text{nzmf} = [\sum_{kl:K < K_f} \hat{E}(k, l) - \sum_l \hat{E}(k=0, l)] / \sum_{kl} \hat{E}(k, l)$. Figure 1 shows both indices as a function of the energy input rate ε and the corresponding value of the nondimensional zonostrophy parameter $R_\beta = 0.7(\varepsilon\beta^2/r^5)^{1/20}$, which was used in previous studies to characterize the emergence and structure of zonal jets in planetary turbulence [11,15]. For ε smaller than a critical value ε_c (corresponding to $R_\beta = 1.64$), the turbulent flow is homogeneous and remains translationally invariant in both directions. When $\varepsilon > \varepsilon_c$,

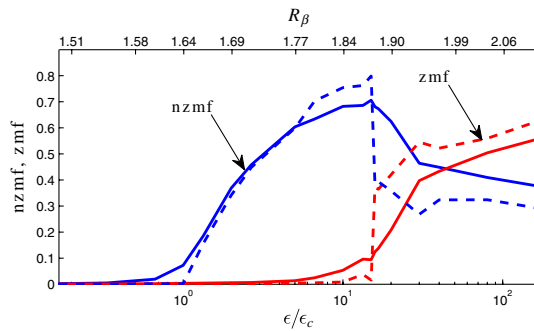


FIG. 1 (color online). The zmf (red lines) and nzmf (blue lines) indices as a function of $\varepsilon/\varepsilon_c$ and R_β for the nonlinear (solid lines) and SSST (dashed lines) integrations. The critical ε_c is the energy input rate at which the SSST predicts structural instability of the homogeneous turbulent state. Zonal jets emerge for $\varepsilon > \varepsilon_{nl}$, with $\varepsilon_{nl} = 15.9\varepsilon_c$.

the translational symmetry of the flow is broken and non zonal structures form with scales larger than the scale of the forcing.

The time averaged power spectrum, shown in Fig. 2(a) for $\varepsilon = 2.6\varepsilon_c$, has pronounced peaks at $(|k|, |l|) = (1, 5)$ that correspond to coherent structures propagating westward [cf. Figs. 3(a) and 3(b)] with approximately the Rossby wave phase speed for this wave. However, at larger ε the propagation speed of these structures departs from that of Rossby waves. For $\varepsilon > \varepsilon_{nl}$ (corresponding to $R_\beta = 1.88$), robust zonal jets emerge. For example, the peaks at $(k, |l|) = (0, 3)$ in the spectrum of Fig. 2(b) correspond to coherent zonal jets [cf. Figs. 3(c) and 3(d)]. From Fig. 1 we see that while the jets contain over half of the total energy, substantial power remains in nonzonal structures.

In this Letter we address the emergence of these nonzonal structures, called satellite modes [8] or zonons [10,11], and assess their effect on jet formation using another interpretation of SSST. SSST describes the statistical dynamics of the first two equal time cumulants of Eq. (1). The first cumulant is $Z(\mathbf{x}, t) \equiv \langle \zeta \rangle$ (the brackets denote an ensemble average) and the second cumulant $C(\mathbf{x}_1, \mathbf{x}_2, t) \equiv \langle \zeta'_1 \zeta'_2 \rangle$ is a function of the vorticity deviation $\zeta'_i = \zeta_i - Z_i$ at the two points $\mathbf{x}_i = (x_i, y_i)$ ($i = 1, 2$). It can be shown from (1) that the equations for the evolution of the cumulants are

$$\begin{aligned} \partial_t Z + UZ_x + V(\beta + Z_y) + rZ + \nu\Delta^2 Z \\ = \partial_x (\partial_{y_1} \Delta_2^{-1} C)_{\mathbf{x}_1=\mathbf{x}_2} - \partial_y (\partial_{x_1} \Delta_2^{-1} C)_{\mathbf{x}_1=\mathbf{x}_2}, \end{aligned} \quad (2a)$$

$$\partial_t C = (A_1 + A_2)C + \Xi, \quad (2b)$$

where

$$\begin{aligned} A_i = -U_i \partial_{x_i} - V_i \partial_{y_i} - (\beta + Z_{y_i}) \partial_{x_i} \Delta_i^{-1} \\ + Z_{x_i} \partial_{y_i} \Delta_i^{-1} - r - \nu \Delta_i^2 \end{aligned} \quad (3)$$

acts at $\mathbf{x}_i = (x_i, y_i)$ and governs the linear dynamics about the instantaneous mean flow $\mathbf{U} = [U, V] = [-\partial_y \langle \psi \rangle, \partial_x \langle \psi \rangle]$. In (2b), Ξ contains the covariance of the external forcing and terms related to third order

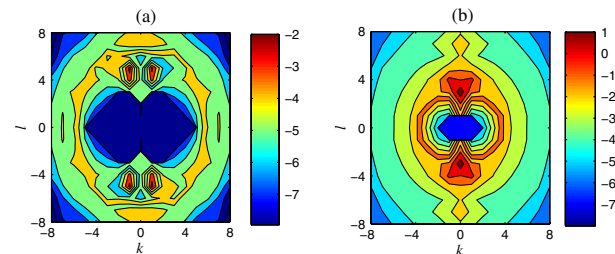


FIG. 2 (color online). Energy power spectra, $\log[\hat{E}(k, l)]$, obtained from nonlinear simulation at (a) $\varepsilon/\varepsilon_c = 2.6$ and (b) $\varepsilon/\varepsilon_c = 30$. In (a) the flow is dominated by a $(|k|, |l|) = (1, 5)$ nonzonal coherent structure. In (b) the flow is dominated by a coherent zonal flow at $(k, |l|) = (0, 3)$.

cumulants. A second order closure is obtained if the third order cumulant is ignored and Ξ is set to be the spatial covariance of the stochastic forcing f . In most earlier studies of SSST, the ensemble average was assumed to represent a zonal average. However, with this interpretation the nonzonal waves are treated as incoherent and their emergence and characteristics cannot be studied. In this Letter, we adopt the more general interpretation introduced to study the emergence of non-zonal structure in baroclinic turbulence [23,33], that the ensemble average represents a Reynolds average with the ensemble mean representing coarse graining. With this interpretation of the ensemble mean, Eq. (2) provides the statistical dynamics of the interaction of the ensemble average field, which can be a zonal or a nonzonal coherent structure, with the fine-grained field, represented in the theory through its covariance C . The fixed points of the SSST dynamics define ideal equilibria that are formally realizable only in the infinite ensemble limit. However, we show here that these equilibria manifest

in actual nonlinear simulations (cf. also [27]). When these equilibria become unstable, a structural reorganization of the turbulence occurs and the turbulent flow bifurcates to a different attractor.

The SSST system (2) has for $\nu = 0$ the equilibrium

$$U^E = V^E = 0, \quad C^E = \Xi/(2r), \quad (4)$$

that has zero large scale flow and a homogeneous eddy field with spatial covariance dictated from the forcing. We now investigate the stability of this equilibrium as a function of the energy input rate ε and the characteristics of the equilibrated unstable structures and relate the outcome of the analysis to the results in the nonlinear simulations of (1). The stability of the homogeneous equilibrium (4) is assessed by introducing perturbations $[\delta Z, \delta C] = [\delta Z_{nm}, \delta C_{nm}]e^{in(x_1+x_2)/2+im(y_1+y_2)/2}e^{\sigma t}$ in Eq. (2) linearized about equilibrium (4) and calculating the eigenvalue σ . It can be shown that σ satisfies the nondimensional equation

$$\frac{\tilde{\varepsilon} K_f}{2\pi \Delta K_f} \sum_{k,l} \frac{(\tilde{m} \tilde{k} - \tilde{n} \tilde{l})[\tilde{n} \tilde{m}(\tilde{k}_+^2 - \tilde{l}_+^2) + (\tilde{m}^2 - \tilde{n}^2)\tilde{k}_+\tilde{l}_+](1 - \tilde{N}^2/\tilde{K}^2)}{2i\tilde{k}_+(\tilde{k}_+\tilde{n} + \tilde{l}_+\tilde{m}) - i\tilde{n}(\tilde{K}^2 + \tilde{K}_s^2)/2 + (\tilde{\sigma} + 2)\tilde{K}^2\tilde{K}_s^2} = (\tilde{\sigma} + 1)\tilde{N}^2 - i\tilde{n}, \quad (5)$$

where $(\tilde{n}, \tilde{m}, \tilde{k}, \tilde{l}) = (n, m, k, l)r/\beta$, $\tilde{\sigma} = \sigma/r$ are the non-dimensional wave numbers and growth rate, respectively, $\tilde{K}^2 = \tilde{k}^2 + \tilde{l}^2$, $\tilde{K}_s^2 = (\tilde{k} + \tilde{n})^2 + (\tilde{l} + \tilde{m})^2$, $\tilde{N}^2 = \tilde{n}^2 + \tilde{m}^2$, $\tilde{k}_+ = \tilde{k} + \tilde{n}/2$, $\tilde{l}_+ = \tilde{l} + \tilde{m}/2$, and the summation is over integer values of (k, l) satisfying $|\tilde{K} - (K_f r/\beta)| < \Delta K_f r/\beta$ [34]. The nondimensional energy input rate $\tilde{\varepsilon} = \varepsilon \beta^2/r^5$,

which is the bifurcating parameter in this Letter, is related to the zonostrophy parameter through $R_\beta = 0.7\tilde{\varepsilon}^{1/20}$. For $n = 0$, Eq. (5) reduces to the equation that determines the emergence of zonal flows [25,35].

For small values of the energy input rate $\tilde{\varepsilon}$, the homogeneous state is stable [i.e., $\text{Re}(\sigma) < 0$ for all n, m]. When $\tilde{\varepsilon}$ exceeds a critical $\tilde{\varepsilon}_c$, the homogeneous flow becomes SSST unstable and coherent structures emerge. The critical $\tilde{\varepsilon}_c$ is defined as $\min_{(n,m)} \tilde{\varepsilon}_t$, where $\tilde{\varepsilon}_t$ is the energy input rate that renders wave numbers (n, m) neutral [$\text{Re}(\sigma) = 0$]. The critical $\tilde{\varepsilon}_c$ depends in general on the forcing characteristics, and for the ring forcing at $K_f = 8$, $\tilde{\varepsilon}_c = 2.48 \times 10^7$ or $R_\beta = 1.64$ [36]. The growth rates as a function of the integer valued wave numbers (n, m) of the structure are shown in Fig. 4. For $\varepsilon/\varepsilon_c = 2.6$, the structure with the largest growth rate is nonzonal with $(|n|, |m|) = (1, 5)$ and has $\text{Im}(\sigma) > 0$, implying retrograde propagation of the

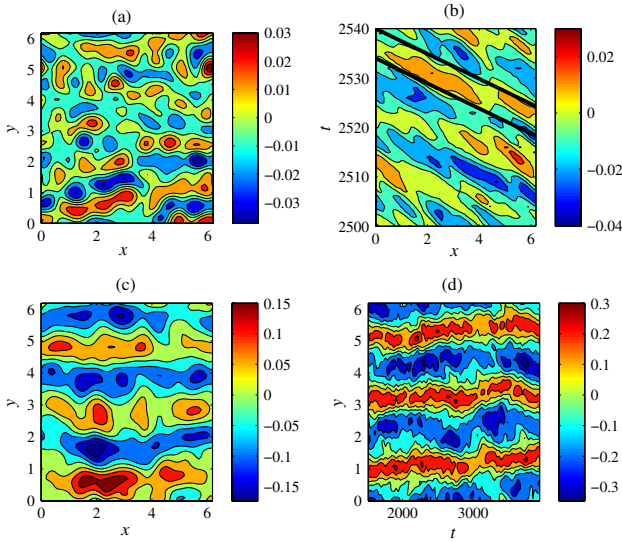


FIG. 3 (color online). (a) Snapshot of the stream function $\psi(x, y, t)$ and (b) Hovmöller diagram of $\psi(x, y = \pi/4, t)$ obtained from nonlinear simulation at $\varepsilon/\varepsilon_c = 2.6$. The thick lines in (b) correspond to the phase speed obtained from Eq. (5). (c) Snapshot of the stream function $\psi(x, y, t)$ and (d) Hovmöller diagram of the x -averaged $\psi(y, t)$ obtained from nonlinear simulation at $\varepsilon/\varepsilon_c = 30$.

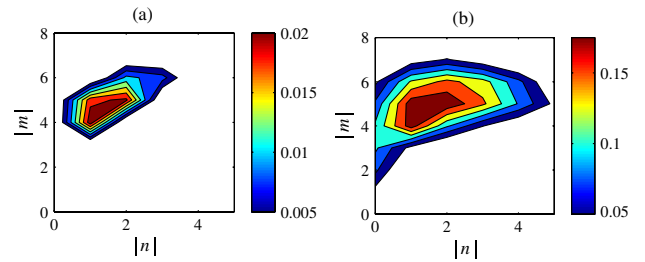


FIG. 4 (color online). The growth rate $\text{Re}(\sigma)$ as a function of the integer valued $|n|, |m|$ for (a) $\varepsilon/\varepsilon_c = 2.6$ and (b) $\varepsilon/\varepsilon_c = 30$ [only positive values of $\text{Re}(\sigma)$ are shown]. Unstable waves with $|n| > 0$ have $\text{Im}(\sigma) > 0$ corresponding to retrograde propagation.

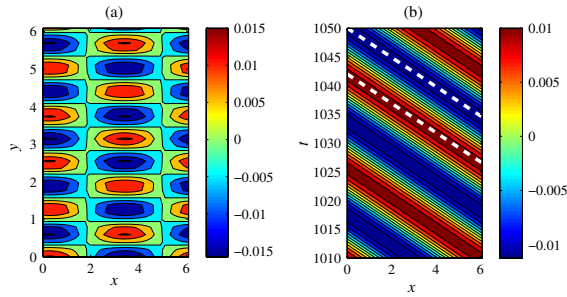


FIG. 5 (color online). (a) Snapshot of $\psi(x, y, t)$ and (b) Hovmöller diagram of $\psi(x, y = \pi/4, t)$ of a SSST integration at $\varepsilon/\varepsilon_c = 2.6$. The thick dashed lines show the phase speed obtained from Eq. (5).

eigenstructure. Note also that for this energy input rate, the zonal flows ($n = 0$) are SSST stable and jets are not expected to form. For $\varepsilon/\varepsilon_c = 30$, both stationary zonal jets [$\text{Im}(\sigma) = 0$] and retrograde propagating nonzonal structures are unstable, but the zonal jets have smaller growth rates compared to the nonzonal structures [37]. Numerical integration of the SSST system (2) shows that for $\varepsilon > \varepsilon_c$ the unstable structures equilibrate at finite amplitude after an initial period of exponential growth. Figure 5(a) shows the equilibrium structure with the largest domain of attraction, when $\varepsilon/\varepsilon_c = 2.6$. This structure coincides with the finite amplitude equilibrium of the fastest growing $(|n|, |m|) = (1, 5)$ eigenfunction and propagates as illustrated in Fig. 5(b) in the retrograde direction with a speed approximately equal to the phase speed of this unstable eigenfunction. A proxy for the amplitude of these equilibrated structures are the zmf and nzmf indices that are calculated for the SSST integrations and are shown in Fig. 1. As the energy input rate increases, the nonzonal structures equilibrate at larger amplitudes. However, for $\varepsilon > \varepsilon_{nl}$, the equilibria with the largest domain of attraction are zonal jets and the flow is dominated by these structures (cf. Fig. 1).

The results of the SSST analysis are now compared to nonlinear simulations. The stability analysis accurately predicts the critical ε_c for emergence of nonzonal structures in the nonlinear simulations as shown in Fig. 1. The finite amplitude equilibria obtained when $\varepsilon > \varepsilon_c$ also correspond to the dominant structures in the nonlinear simulations. For $\varepsilon/\varepsilon_c = 2.6$, the spectra in the nonlinear simulations show significant power at $(|n|, |m|) = (1, 5)$, corresponding to the SSST structure with the largest domain of attraction. Remarkably, the phase speed of these waves observed in the nonlinear simulations and the amplitude of these structures as illustrated by the nzmf index are approximately equal to the phase speed and amplitude of the corresponding SSST translating equilibrium structure (cf. Figs. 1, 3, and 5). For $\varepsilon > \varepsilon_{nl}$, in both nonlinear and SSST simulations zonal jets emerge and the power of the nonzonal structures is reduced. Comparison of the number of jets and their amplitude between the SSST and the nonlinear simulations also shows good agreement (not

shown). This demonstrates that the SSST system can predict the amplitude and characteristics of both the nonzonal and the zonal structures that emerge in the turbulent flow.

While the regime transition that occurs at ε_c is predicted by the stability equation (5), the second transition, which is associated with the emergence of zonal flows and occurs at ε_{nl} , is more intriguing. Equation (5) predicts that the zonal structures become unstable at $\varepsilon_{sz} = 4\varepsilon_c < \varepsilon_{nl}$. In previous studies of SSST dynamics restricted to the interaction between zonal flows and turbulence, these initially unstable structures were found to equilibrate at finite amplitude and as a result the predictions of the SSST theory did not agree with nonlinear simulations [25,27]. Preliminary calculations show that, within the context of this generalized SSST analysis that takes into account the dynamics of nonzonal structures as well, these equilibria are found to be saddles that are stable to zonal but unstable to nonzonal perturbations. The threshold for the emergence of jets in the SSST and in the nonlinear simulations is therefore determined as the energy input rate at which a SSST stable, finite amplitude zonal jet equilibrium exists. It is worth noting that a method to correctly obtain this threshold ε_{nl} even within the context of SSST employed with a zonal average has been recently developed [27].

In summary, we presented a theory that shows that large scale structure in barotropic turbulence arises through systematic self-organization of the turbulent Reynolds stresses, in the absence of cascades. The theory allowed the determination of conditions for the emergence of coherent structures in homogeneously forced flows and we have demonstrated, through comparison with nonlinear simulations, that it predicts both the emergence and the finite amplitude equilibration of these structures. An advance made in this Letter is the development of the theoretical framework that accounts for the emergence of westward propagating nonzonal (or lattice) states in turbulence and for their effect on the zonal jet dynamics. The relation of these states to westward propagating vortex rings in the ocean and coherent vortices in planetary atmospheres will be the subject of future research.

This research was supported by the EU FP-7 under the PIRG03-GA-2008-230958 Marie Curie Grant. The authors acknowledge the hospitality of the Aspen Center for Physics supported by the NSF (under Grant No. 1066293), where part of this work was done. The authors would also like to thank Navid Constantinou and Brian Farrell for fruitful discussions.

*nikos.bakas@gmail.com

†pjioannou@phys.uoa.gr

- [1] A. R. Vasavada and A. P. Showman, *Rep. Prog. Phys.* **68**, 1935 (2005).
- [2] P. H. Diamond, S. I. Itoh, K. Itoh, and T. S. Hahm, *Plasma Phys. Controlled Fusion* **47**, R35 (2005).

- [3] M.G. Shats, H. Xia, and M. Yokoyama, *Plasma Phys. Controlled Fusion* **48**, S17 (2006).
- [4] H. Xia, M.G. Shats, and H. Punzmann, *Phys. Rev. Lett.* **97**, 255003 (2006).
- [5] G.P. Williams, *J. Atmos. Sci.* **35**, 1399 (1978).
- [6] G.K. Vallis and M.E. Maltrud, *J. Phys. Oceanogr.* **23**, 1346 (1993).
- [7] B. Nadiga, *Geophys. Res. Lett.* **33**, L10601 (2006).
- [8] S. Danilov and D. Gurarie, *Phys. Fluids* **16**, 2592 (2004).
- [9] B.H. Galperin, S. Sukoriansky, N. Dikovskaya, P. Read, Y. Yamazaki, and R. Wordsworth, *Nonlinear Proc. Geophys.* **13**, 83 (2006).
- [10] S. Sukoriansky, N. Dikovskaya, and B. Galperin, *Phys. Rev. Lett.* **101**, 178501 (2008).
- [11] B.H. Galperin, S. Sukoriansky, and N. Dikovskaya, *Ocean Dyn.* **60**, 427 (2010).
- [12] P.B. Rhines, *J. Fluid Mech.* **69**, 417 (1975).
- [13] S. Nazarenko and B. Quinn, *Phys. Rev. Lett.* **103**, 118501 (2009).
- [14] D.G. Dritchel and M.E. McIntyre, *J. Atmos. Sci.* **65**, 855 (2008).
- [15] R.K. Scott and D.G. Dritchel, *J. Fluid Mech.* **711**, 576 (2012).
- [16] A.E. Gill, *Geophysical Fluid Dynamics* **6**, 29 (1974).
- [17] C. Connaughton, B. Nadiga, S. Nazarenko, and B. Quinn, *J. Fluid Mech.* **654**, 207 (2010).
- [18] W.A. Robinson, *J. Atmos. Sci.* **63**, 2109 (2006).
- [19] F. Bouchet and A. Venaille, *Phys. Rep.* **515**, 227 (2012).
- [20] F. Bouchet and E. Simonnet, *Phys. Rev. Lett.* **102**, 094504 (2009).
- [21] B.F. Farrell and P.J. Ioannou, *J. Atmos. Sci.* **60**, 2101 (2003).
- [22] B.F. Farrell and P.J. Ioannou, *J. Atmos. Sci.* **64**, 3652 (2007).
- [23] J. Bernstein and B.F. Farrell, *J. Atmos. Sci.* **67**, 452 (2010).
- [24] J.B. Marston, E. Conover, and T. Schneider, *J. Atmos. Sci.* **65**, 1955 (2008).
- [25] K. Srinivasan and W.R. Young, *J. Atmos. Sci.* **69**, 1633 (2012).
- [26] J.B. Marston, *Annu. Rev. Condens. Matter Phys.* **3**, 285 (2012).
- [27] N.C. Constantinou, P.J. Ioannou, and B.F. Farrell, [arXiv:1208.5665](https://arxiv.org/abs/1208.5665).
- [28] S.M. Tobias and J.B. Marston, *Phys. Rev. Lett.* **110**, 104502 (2013).
- [29] M. Cross and H. Greenside, *Pattern Formation and Dynamics in Nonequilibrium Systems* (Cambridge University Press, Cambridge, England, 2009), p. 489.
- [30] J.B. Parker and J.A. Krommes, [arXiv:1301.5059v1](https://arxiv.org/abs/1301.5059v1).
- [31] B.F. Farrell and P.J. Ioannou, *J. Atmos. Sci.* **65**, 3353 (2008).
- [32] B.F. Farrell and P.J. Ioannou, *Phys. Plasmas* **16**, 112903 (2009).
- [33] J. Bernstein, Ph.D. thesis, Harvard University, 2009.
- [34] Hyperdiffusion can be readily included in Eq. (5) in order to obtain correspondence with the nonlinear simulations.
- [35] N.A. Bakas and P.J. Ioannou, *J. Fluid Mech.* **682**, 332 (2011).
- [36] It can be shown that $\tilde{\epsilon}_c$ is a decreasing function of K_f with a minimum value occurring at $\lim_{K_f \rightarrow \infty} \tilde{\epsilon}_c = 23$ or $R_\beta = 0.82$.
- [37] This is always true for $\beta > 4.5rK_f$ for the given isotropic forcing.